

# Direct numerical simulation tests of eddy viscosity in two dimensions

A. Chekhlov and S. A. Orszag

*Program in Applied and Computational Mathematics, Princeton University, Princeton, New Jersey 08544*

S. Sukoriansky

*Department of Mechanical Engineering, Ben-Gurion University of the Negev, Beer-Sheva 84105, Israel*

B. Galperin

*Department of Marine Science, University of South Florida, St. Petersburg, Florida 33701*

I. Staroselsky

*Cambridge Hydrodynamics, Inc., P.O. Box 1403, Princeton, New Jersey 08542*

(Received 14 September 1993; accepted 29 December 1993)

Two-parametric eddy viscosity (TPEV) and other spectral characteristics of two-dimensional (2-D) turbulence in the energy transfer subrange are calculated from direct numerical simulation (DNS) with  $512^2$  resolution. The DNS-based TPEV is compared with those calculated from the test field model (TFM) and from the renormalization group (RG) theory. Very good agreement between all three results is observed.

Two-dimensional (2-D) incompressible turbulent flows are described by the vorticity equation:

$$\frac{\partial \zeta}{\partial t} + \frac{\partial(\nabla^{-2} \zeta, \zeta)}{\partial(x, y)} = \nu_0 \nabla^2 \zeta, \quad (1)$$

where  $\zeta$  is fluid vorticity and  $\nu_0$  is molecular viscosity. It is well known that the existence of inviscid invariants  $\int d^2x \zeta^{2n}$  of (1) results in the flux of energy towards the largest spatial scales. The presence of this inverse cascade complicates the large-scale description of 2-D flows and requires refinement of the classical hydrodynamic notion of ‘‘eddy viscosity.’’ The concept of eddy viscosity is well defined for three-dimensional (3-D) turbulent flows, where energy cascades towards the smallest flow scales where it is dissipated. To achieve an adequate coarse-grained description of 3-D flow, one can introduce increased ‘‘effective’’ viscosity which accounts for the unresolved dissipation.

In 2-D flows, the inverse flux of energy at large scales and enstrophy dissipation at small scales make the eddy viscosity concept more subtle. It was argued by Kraichnan<sup>1</sup> that a 2-D eddy viscosity should include two parameters: a cutoff wave number  $k_c$  (which essentially determines the size of the coarse grain), and the wave number of a given mode,  $k$ . The two-parameter eddy viscosity (TPEV), denoted by  $\nu(k|k_c)$ , describes the energy exchange between a given resolved vorticity mode with the wave number  $k$  and all subgrid, or unresolved, modes with  $k > k_c$ ; it provides correct account for the energy and enstrophy fluxes between resolved and unresolved scales. The TPEV is derived from the evolution equation for the spectral enstrophy density  $\Omega(k, t) \equiv \pi k \langle \zeta(\mathbf{k}, t) \zeta(-\mathbf{k}, t) \rangle$ , where  $\langle \dots \rangle$  denotes averaging over thin circular shells:

$$(\partial_t + 2\nu k^2) \Omega(k, t) = T_\Omega(k, t). \quad (2)$$

Here, the enstrophy transfer function  $T_\Omega(k, t)$  is given by

$$T_\Omega(k, t) = 2\pi k \int_{\mathbf{p}+\mathbf{q}=\mathbf{k}} \frac{\mathbf{p} \times \mathbf{q}}{p^2} \times \langle \zeta(\mathbf{p}, t) \zeta(\mathbf{q}, t) \zeta(-\mathbf{k}, t) \rangle [d\mathbf{p} d\mathbf{q} / (2\pi)^2]. \quad (3)$$

Assuming that the system is in statistical steady state and extending integration in (3) only over all such triangles  $(\mathbf{k}, \mathbf{p}, \mathbf{q})$  that  $p$  and/or  $q$  are greater than  $k_c$ , one defines the two-parametric transfer  $T_\Omega(k|k_c)$  and TPEV:<sup>1</sup>

$$\nu(k|k_c) = -T_\Omega(k|k_c) / 2k^2 \Omega(k). \quad (4)$$

In a wide class of quasinormal approximations<sup>2</sup> the transfer  $T_\Omega(k|k_c)$  in two dimensions is given by

$$T_\Omega(k|k_c) = \frac{2k}{\pi} \iint_{\Delta} \Theta_{-k,p,q} (p^2 - q^2) \sin \alpha \times \left[ \frac{p^2 - q^2}{p^3 q^3} \Omega(p) \Omega(q) - \frac{k^2 - q^2}{k^3 q^3} \Omega(q) \Omega(k) + \frac{k^2 - p^2}{k^3 p^3} \Omega(p) \Omega(k) \right] dp dq, \quad (5)$$

where  $\Theta_{-k,p,q}$  is the triad relaxation time. Here, the angle  $\alpha$  is formed by the vectors  $\mathbf{p}$  and  $\mathbf{q}$ , and  $\iint_{\Delta}$  denotes integration over the area defined above (4).

The main difference between various spectral closure models is in specification of  $\Theta_{-k,p,q}$ . In Ref. 1,  $T_\Omega(k|k_c)$  was evaluated using TFM. It was found that TPEV is a sign-changing function of the form  $\nu(k|k_c) = |\nu(0|k_c)| N(k/k_c)$ , with  $\nu(0|k_c) < 0$ ,  $N(0) = -1$ , and  $N(1) \approx 2.1$ . The derivation of  $\Theta_{-k,p,q}$  using the RG theory was given in Ref. 3 and adapted for 2-D isotropic and anisotropic turbulence in Refs. 4 and 5, respectively. In the present work, we compare  $\nu(k|k_c)$  for the inverse energy cascade regime calculated from DNS data with those predicted by TFM and the RG theory. Let us mention that for the enstrophy transfer subrange of 2-D turbulence, eddy viscosity was calculated by Maltrud and Vallis.<sup>6</sup>

We solve Eq. (1) numerically in a periodic box  $2\pi \times 2\pi$  using  $512^2$  Fourier modes, utilizing a Fourier–Galerkin pseudospectral spatial approximation with implicit Adams-type second-order stiffly stable time-stepping scheme.<sup>7</sup> To increase the effective inertial range, mode-selective

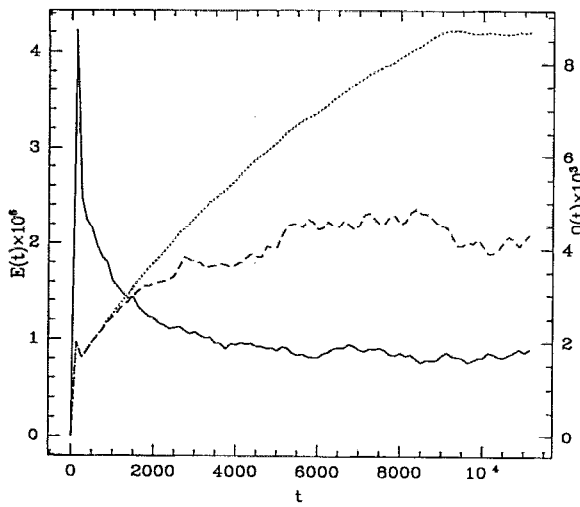


FIG. 1. Evolution of the total energy  $E(k)$  (dotted line) and enstrophy  $\Omega(k)$  (solid line) towards the steady state. Dashed line denotes the total energy with the first 6 modes excluded.

hyperviscosity<sup>8</sup>  $\nu(k) = \nu_L(k) + \nu_S(k) = A_L k^{-10} + A_S k^{14}$  has been introduced in the vorticity equation (1) instead of the molecular viscosity.

The white noise, high wave number forcing was introduced in three consecutive wave numbers,  $k_f - 1$ ,  $k_f$ , and  $k_f + 1$ , where  $k_f = 98$ .

In Figs. 1(a) and 1(b) we plot the total energy  $E_{\text{tot}}(t) = \int_0^{+\infty} k^{-2} \Omega(k, t) dk$  and enstrophy  $\Omega_{\text{tot}}(t) = \int_0^{+\infty} \Omega(k, t) dk$ . One can see that the energy grows with time and eventually tends to reach a steady state. However, the drift towards the energy steady state is significantly slower than towards that of the enstrophy. Defining the RMS velocity as  $V_{\text{RMS}}^2 = \sum_{\mathbf{k}} |\mathbf{u}(\mathbf{k})|^2$  and the characteristic turnover time of the largest eddies as  $\tau_{tu} = 2\pi/V_{\text{RMS}}$ , we infer that a steady state for the total enstrophy was achieved after about  $1.2\tau_{tu}$ , while about  $5\tau_{tu}$  were required to attain a steady

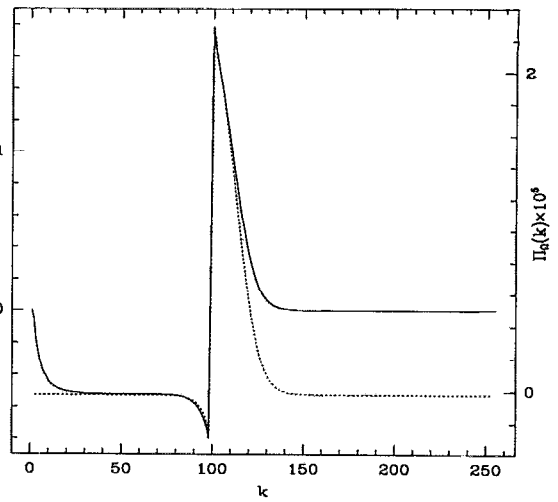


FIG. 3. The energy flux  $\Pi_E(k)$  (solid line) and the enstrophy flux  $\Pi_\Omega(k)$  (dotted line).

state for the total energy. Note however that all the modes with  $k > 5$  have reached the steady state after  $t \approx 2\tau_{tu}$ , and only the largest modes were still developing. The results presented below pertain to the integration time  $t \leq 10^4$ , before the energy saturates at low wave numbers.

In Fig. 2 we plot the time-averaged energy spectrum after about  $5\tau_{tu}$ . The inertial range  $E \propto k^{-x}$  extends over more than a decade in wave number space. Mean square line-fitting over the interval  $k \in (12, 50)$  gives the scaling exponent close to the Kolmogorov value of  $\frac{5}{3}$ . Note that good agreement with the Kolmogorov scaling in the energy sub-range has been reported recently in Ref. 6 for  $256^2$  simulations and in Ref. 9 for very high resolution simulations with  $2048^2$  Fourier modes. In Fig. 2 we also plot a compensated energy spectrum,  $k^{5/3} \epsilon^{-2/3} E(k)$ , where  $\epsilon$  is the energy transfer rate. The value of the Kolmogorov constant calcu-

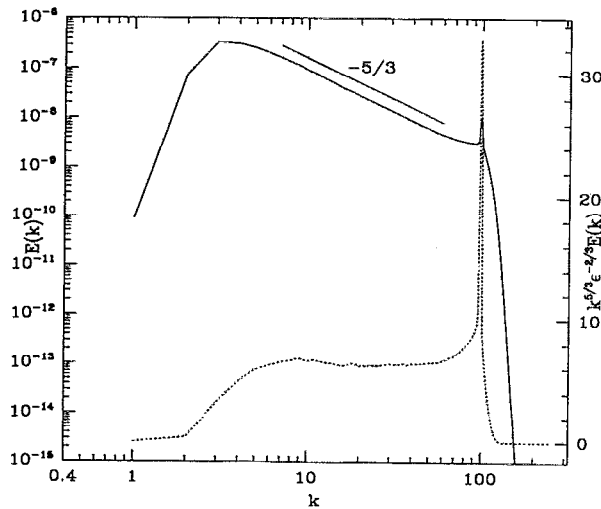


FIG. 2. Energy spectrum  $E(k)$  (solid line) and compensated energy spectrum  $E(k)k^{5/3}\epsilon^{-2/3}$  (dotted line).

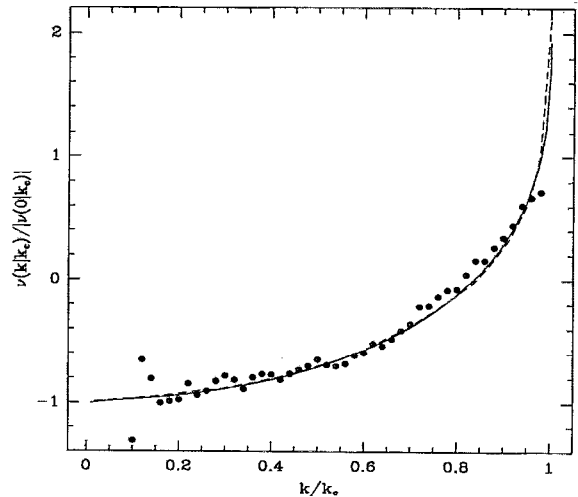


FIG. 4. Normalized two-parametric eddy viscosity from DNS (dots), from TFM (dashed line), and from RG (solid line).

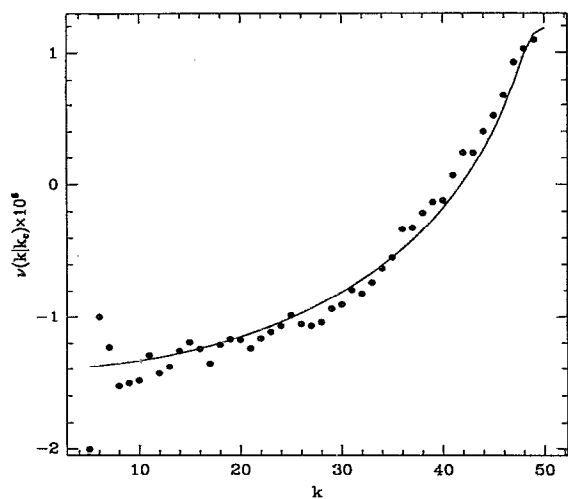


FIG. 5. Actual two-parametric eddy viscosity from DNS (dots) and from RG (solid line). In RG calculations, the energy spectrum for  $k < 5$  was corrected in accordance with the DNS results (Fig. 2).

lated from this data is about  $C_k = 6.2$ , in reasonable agreement with 5.8, calculated from DNS in Ref. 10 using the  $256^2$  resolution and 6.69, obtained analytically in Ref. 11 on the basis of TFM.

In Figs. 3(a) and 3(b) we plot the  $k$ -dependent energy and enstrophy flux functions, defined as  $\Pi_E(k) = \int_0^k T_\Omega(n) n^{-2} dn$  and  $\Pi_\Omega(k) = \int_0^k T_\Omega(n) dn$ , respectively. As expected, an inverse energy cascade with constant transfer rate  $\epsilon$  develops for  $k < k_f = 98$ . The resolution employed in this study was insufficient to detect a well defined enstrophy transfer range. The flux of enstrophy in the energy subrange,  $k < k_f$ , is zero. Figures 3(a) and 3(b) indicate that the numerical scheme used conserves both total energy and enstrophy.

We have calculated  $k$  and  $k_c$ -dependent enstrophy transfer function  $T_\Omega(k|k_c)$  in (4) by computing the third-order vorticity cumulants in (3) extending the integration only over those  $\mathbf{p}$  and  $\mathbf{q}$  that either  $p \geq k_c$  or  $q \geq k_c$ . We have set  $k_c = 50$ , well inside the energy inertial subrange.

The DNS-inferred normalized TPEV [viz., the function  $N(k/k_c) = \nu(k|k_c)/\nu(0|k_c)$ ] is plotted in Fig. 4, along with the TFM-based<sup>1</sup> and RG-based<sup>4</sup> analytical predictions. The agreement between the DNS-based results and the TFM and RG theories is very good over the entire energy transfer range, up to the wave numbers close to  $k_c$ , where the DNS data saturates, while TFM and RG curves exhibit sharp cusp. The physics leading to this cusp is as follows. As closer  $k$  approaches  $k_c$ , as more elongated triads with either  $p$  or  $q \ll k_c$  become involved in the energy exchange between the mode  $k$  and the subgrid scale modes. The contribution from these triads results in the cusp behavior of the theoretical TPEV. However, in finite box DNS with large-scale energy

removal, the energy of small wave number modes is reduced (see Fig. 2), which implies that instead of the sharp growth, the TPEV should saturate at  $k \rightarrow k_c$ . To illustrate and quantify this explanation, we recalculated the RG-based TPEV with the enstrophy spectrum in (5) corrected at  $k \leq 5$  according to Fig. 2. In Fig. 5, we compare the DNS- and RG-based TPEV in their actual values, whereas the RG calculations were based upon the value of  $\epsilon$  found from DNS. The agreement between the two is very good. Also, we have calculated TPEV for  $k_c = 35, 45$ , and  $55$  and found that the DNS-inferred TPEV scales with  $k_c^{-4/3}$ , in full agreement with the Kolmogorov and Richardson laws. At all values of  $k_c$  tested an equally good agreement between DNS data and RG predictions was observed.

The good agreement demonstrated in Figs. 4 and 5 provides an indirect validation of TFM and RG results for isotropic 2-D turbulence in the energy transfer subrange.

## ACKNOWLEDGMENTS

The authors would like to thank Eric Jackson for valuable help with some programming issues, and Robert Kraichnan who kindly provided his data for TFM-based eddy viscosity. This research has been partially supported by ONR Grant Nos. N00014-92-J-1363, N00014-92-C-0089 and N00014-92-C-0118, NSF Grant No. OCE 9010851, and the Perlstone Center for the Aeronautical Engineering Studies. The computations were performed on the Cray Y-MP of NAVOCEANO Supercomputer Center, Stennis Space Center, Mississippi.

- <sup>1</sup>R. H. Kraichnan, "Eddy viscosity in two and three dimensions," *J. Atmos. Sci.* **33**, 1521 (1976).
- <sup>2</sup>W. D. McComb, *The Physics of Fluid Turbulence* (Oxford Science Publications, London, 1991).
- <sup>3</sup>W. P. Dannevik, V. Yakhot, and S. A. Orszag, "Analytical theories of turbulence and the  $\epsilon$  expansion," *Phys. Fluids* **30**, 2021 (1987).
- <sup>4</sup>I. Staroselsky and S. Sukoriansky, "Renormalization group approach to two-dimensional turbulence and the  $\epsilon$ -expansion for the vorticity equation," in *Advances in Turbulence Studies*, Progress in Astronautics and Aeronautics, edited by H. Branover and Y. Unger (AIAA, Washington, DC, 1993), Vol. 149, p. 159.
- <sup>5</sup>B. Galperin, S. Sukoriansky, and I. Staroselsky, "Eddy Rossby wave frequency in  $\beta$ -plane turbulence," *Phys. Fluids A* **5**, 2083 (1993).
- <sup>6</sup>M. E. Maltrud and G. K. Vallis, "Energy and enstrophy transfer in numerical simulations of two-dimensional turbulence," *Phys. Fluids A* **5**, 1760 (1993).
- <sup>7</sup>G. E. Karniadakis, M. Israeli, and S. A. Orszag, "High-order splitting methods for the incompressible Navier-Stokes equations," *J. Comput. Phys.* **97**, 414 (1991).
- <sup>8</sup>B. Legras, P. Santangelo, and R. Benzi, "High-resolution numerical experiments for forced two-dimensional turbulence," *Europhys. Lett.* **5**, 37 (1988).
- <sup>9</sup>L. M. Smith and V. Yakhot, "Bose condensation and small-scale structure generation in a random force driven 2D turbulence," *Phys. Rev. Lett.* **71**, 352 (1993).
- <sup>10</sup>M. E. Maltrud and G. K. Vallis, "Energy spectra and coherent structures in forced two-dimensional and beta-plane turbulence," *J. Fluid Mech.* **228**, 321 (1991).
- <sup>11</sup>R. H. Kraichnan, "Inertial-range transfer in two- and three-dimensional turbulence," *J. Fluid Mech.* **3**, 47 (1971).